Mass Spectrometric Based Mapping of the Disulfide Bonding Patterns of Integrin α Chains†

Oleg V. Krokhin,[‡,§,||] Keding Cheng,[‡,§] Sandra L. Sousa,[‡,§] Werner Ens,[‡,||] Kenneth G. Standing,[‡,||] and John A. Wilkins*[,‡,§]

Manitoba Centre for Proteomics and Rheumatic Diseases Research Laboratory, Department of Medicine, University of Manitoba, Winnipeg, Manitoba, Canada R3E 3P4, and Time of Flight Laboratory, Department of Physics and Astronomy, University of Manitoba, Winnipeg, Manitoba, Canada R3T 2N2

Received May 6, 2003; Revised Manuscript Received September 15, 2003

ABSTRACT: Integrins are one of the major mediators of cellular adherence. Structurally the component α and *β* chains are characterized by extensive intrachain disulfide bonding. The assignment of these bonds is currently based on homology with the chains of the integrin αIIb*β*3. However, recent crystallographic analysis of the soluble αV*β*3 construct indicates that the αV chain displays bonding patterns different from those predicted for αIIb. In an effort to define the disulfide bonding patterns in integrins, we have used mass spectrometric based approaches to map the human α3, α5, αV, and αIIb. The results indicate that there are differences in the disulfide patterns of the α chains. These do not correlate with the integrin capacity to bind ligands as all integrins used in the present study displayed functional activity. The differences were observed in the bonding patterns linking the heavy (H) and light (L) components of the of the α chains. It was also possible to assign the location in α5 of an additional disulfide bond involving a pair of cysteines not present in αV or αIIb. This second bond between the H and L chains of α5 has not been previously described. These results indicate that not all integrin species display the same disulfide bonding patterns. They also highlight the need for caution in the use of assignments based on sequence homology.

Integrins mediate cellular adherence to a range of ligands including extracellular matrix proteins and cell surface associated cognates (*1*, *2*). Such interactions between integrins and their ligands play an essential role in defining the cellular responses to these interactions (e.g., survival, growth, and differentiation) (*3*). In cell types, such as platelets and leukocytes, the capacity of the integrins to bind ligand is highly regulated (*4*). This property is critical for processes such as thrombus formation, lymphocyte homing, and cellular interactions in which transient targeted adhesive events are required for the generation of platelet aggregates or local immune responses (*5*, *6*).

The structural basis for the regulation of integrin function is presently unknown, but mechanisms involving both affinity and avidity changes have been proposed (*7*−*9*). The initial stage of induction of integrin-mediated leukocyte adhesion appears to be mediated predominantly by changes in integrin avidity, arising in part from changes in integrin mobility within the plasma membrane (*7*, *8*). However, changes in integrin affinity have also been observed often in conjunction with conformational shifts within the integrins (*9*, *10*).

Several observations suggest that integrin disulfide exchange may be involved in aspects of the control of integrin activation. Cellular adhesion mediated by *β*1, *β*2, and *β*3 integrins can be enhanced by bifunctional reducing agents such as DTT[1] (*11*−*14*). These effects are also observed with purified integrins, αIIb*β*3 and α5*β*1, suggesting that the reducing agents are acting directly on the integrins rather than through indirect pathways (*11*, *13*). The demonstration of protein disulfide isomerase on the surface of activated platelets and the ability of inhibitors of PDI to prevent integrin-dependent adhesion suggest that disulfide exchange dependent processes are involved in integrin activation (*15*). Recently, purified integrins have been shown to possess endogenous thiol isomerase (TI) activity, indicating flexibility in the intramolecular disulfide bonding patterns of a single integrin species (*16*). The low- and high-affinity states of the integrin αIIb*β*3 suggest that there are differences in the

† This research was supported by grants from the Canadian Institutes of Health Research (to J.A.W.), the National Institutes of Health (GM59240), and the Natural Sciences and Engineering Research Council of Canada.

* Correspondence should be addressed to this author at the Rheumatic Diseases Research Laboratory, 805 John Buhler Research Centre, 715 McDermot Ave., Winnipeg, Manitoba, Canada R3E 3P4. E-mail: jwilkin@cc.umanitoba.ca. Phone: 204 789 3835. Fax: 204 789 3987.

‡ Manitoba Centre for Proteomics.

§ Rheumatic Diseases Research Laboratory.

|| Time of Flight Laboratory, Department of Physics and Astronomy.

[1] Abbreviations: DTT, dithiothreitol; ESI, electrospray ionization; fwhm, full width at half-maximum; HPLC, high-performance liquid chromatography; MS, mass spectrometry; MS/MS, tandem mass spectrometry; MALDI, matrix-assisted laser desorption ionization; *μ*-LC, micro-liquid chromatography; PDI, protein disulfide isomerase; PNGase F, peptide−*N*-glycosidase F [peptide−N^4-(*N*-acetyl-*β*-glucosaminyl)asparagine amidase, EC 3.5.1.52]; QqTOF, quadrupole/time of flight; TBS, 50 mM Tris, pH 7.4, 150 mM NaCl, 1 mM $MgCl_2$, and 0.1 mM $CaCl_2$; TBS-A, 0.1% bovine serum albumin in TBS; TFA, trifluoroacetic acid; TI, thiol isomerase.

10.1021/bi034726u CCC: $25.00
Published on Web 10/17/2003

numbers of accessible SH groups on the integrins, implying a relationship between functionality and redox status of the molecule (*17*). In the case of αIIbβ3, activation of ligand binding with DTT appears to be associated with rearrangement of intrachain disulfide groups (*18*). Collectively, these observations suggest that disulfide bonds may not be fixed in integrins and that changes in bonding patterns may be associated with different states of integrin activity.

The integrins are type I membrane proteins consisting of a noncovalently linked α and β heterodimer (*1*). In several integrin species the α chains are posttranslationally cleaved to produce a membrane-spanning light chain and a disulfide-linked extracellular heavy chain (*2*). The α and β chains contain a large number of cysteines (e.g., α, 19−35; β, 56). The basis for disulfide assignment in these chains has been by homology with αIIbβ3, which was originally determined by Calvette et al. (*19*, *20*). Recent crystallographic studies of a recombinant form of αVβ3 lacking the cytoplasmic and transmembrane regions indicate that while the observed disulfide patterns are generally consistent with those reported for αIIbβ3, there are some differences (*21*, *22*). These differences were specifically associated with the bond pair between the light and heavy chains of the αV. These results raised the possibility that for integrins disulfide assignment by homology might not be justified. An alternate but not mutually exclusive interpretation might be that the disulfide bonding patterns are flexible and the patterns represent different functional states. These observations highlight the importance of determining integrin disulfide bonding patterns in other integrins.

X-ray crystallography is the method of choice for detailed structural analysis of proteins. However, the approach requires significant quantities of crystallizable protein. Neither of these requirements is necessarily attainable, particularly in the case of membrane proteins. Mass spectrometry provides an alternative method for the analysis of disulfide bonding patterns (*23*−*25*). This capacity is largely associated with the development of matrix-assisted laser desorption/ionization (MALDI) and electrospray ionization (ESI) techniques in the past two decades. The approach offers several potential advantages in that small amounts of material are required and unambiguous assignments can be made using MS or MS/MS. The strategy commonly involves digestion of nonreduced proteins followed by HPLC fractionation and MS (MS/MS) analysis of nonreduced or reduced digests. However, there are no universal recommendations, and often a combination of different methods including partial reduction are employed. The approach has been used to solve complicated cases of disulfide pairing (*23*−*28*).

The present studies were undertaken to characterize the disulfide bonding patterns in the α chains of several different integrins. Our results indicate that MS in conjunction with μ-LC can be used to map disulfide bonds in highly complex proteins such as integrin α chains. This approach also allowed us to determine the location of a previously unassigned disulfide bond that provides a second linkage between the heavy and light components of the α5 integrin chain. Furthermore, we demonstrate that integrin bond assignments cannot necessarily be made on the basis of amino acid sequence homology, highlighting the importance of detailed protein structural analysis.

MATERIALS AND METHODS

Integrin Purification and Characterization. The integrins α3β1, α5β1, and αVβ3 were immunoaffinity purified from human placenta, and αIIbβ3 was isolated from outdated human platelets (*29*, *30*). The integrins were reduced and separated by SDS−PAGE in an 8% gel and stained with colloidal Coomassie blue (Pierce).

Ligand binding was assessed in an ELISA-based assay (*25*). Briefly, purified integrin (1 μg/mL) in TBS (50 mM Tris, pH 7.4, 150 mM NaCl, 1 mM $MgCl_2$, 0.1 mM $CaCl_2$) was added to microtiter wells and incubated overnight at 4 °C. The plates were blocked with 0.1% bovine serum albumin in TBS (TBS-A), and the indicated concentrations of biotinylated fibronectin in A-TBS were added to the wells. The plates were incubated at 37 °C for 3 h and washed extensively with TBS-A containing 0.5% Tween 20, after which alkaline phosphatase conjugated streptavidin was added. The plates were incubated for 1 h at room temperature, and the wells were washed with TBS-A. Substrate was added to the wells, and color was developed. The absorbance of the samples was determined at 405 nm (*29*). Experiments were performed in sextuplicate. The level of nonspecific binding was determined by incubating samples with biotinylated fibronectin in the presence of a 100-fold excess of unlabeled fibronectin. Results are expressed as the means of the samples after subtraction of the nonspecific background at each concentration of ligand.

Disulfide Analysis. Preliminary studies included peptide mapping to confirm integrin identity. For this purpose integrin samples were fully reduced with 10 mM DTT (30 min at 56 °C), alkylated with 50 mM iodoacetamide in the absence of denaturants (30 min, room temperature in the dark), dialyzed against 50 mM ammonium bicarbonate, deglycosylated for 12 h at 37 °C with 0.1 unit/μL PNGase F (Roche), and digested with trypsin (excision grade, Calbiochem). The resulting digests were either directly analyzed by MALDI MS or HPLC fractionated prior to MS.

For the assignment of disulfide bonds purified integrins were dialyzed against 50 mM NH_4HCO_3, deglycosylated with PNGase F, and digested with trypsin (1/50 substrate to enzyme ratio). Full reduction was achieved by treating the integrin digests for 30 min at 56 °C in the presence of 5 mM DTT in 50 mM NH_4HCO_3. Alkylation was carried out at room temperature in the presence of 30 mM iodoacetamide. Tryptic fragments carrying disulfide bonds disappeared after such a treatment, and new ones appeared having Cys residues alkylated with iodoacetamide. The resulting tryptic fragments were analyzed by MALDI mass spectrometry with and without prior LC fractionation or by tandem mass spectrometry of the daughter ions following low-energy collision-induced dissociation of the mass-selected tryptic fragment (MS/MS).

In those cases where partial reduction was sought, integrins were reduced under mild conditions (3 mM DTT, 3 min on ice), alkylated with 25 mM iodoacetamide, extensively dialyzed against 50 mM ammonium bicarbonate, completely reduced, alkylated with iodoacetic acid, deglycosylated with PNGase F, and digested with trypsin. Control experiments for this study included the same sample preparation steps except prior alkylation in mild conditions. This experiment was undertaken so as to detect the presence of free cysteines

on purified integrins to distinguish them from those formed after reduction in mild conditions.

All digests were either analyzed directly by MALDI MS or MS/MS or subjected to μ-HPLC fractionation followed by MS or MS/MS analysis.

Chromatography. Chromatographic separations of integrin digests were performed using an Agilent 1100 Series μ-LC system. Samples, 5 μL in 0.1% TFA, were injected onto capillary columns (150 μm × 150 mm) packed with Vydac 218 TP C18 (5 μm diameter) and eluted (4 μL/min) with a linear gradient of 1−90% acetonitrile (0.1% TFA) in 70 min. Column effluent was mixed on-line with MALDI matrix solution (0.5 μL/min), and fractions were deposited on the MALDI target at 1 min intervals. MALDI matrix solution was prepared by dissolving 2,5-dihydroxybenzoic acid (150 mg/mL) (Sigma) in deionized water and acetonitrile (1:1). The fractions were air-dried on the target and subjected to MALDI QqTOF MS (MS/MS) analysis. Preliminary studies indicated that the bulk of the retained peptides eluted in a 40 min gradient; thus 40 fractions were collected.

Mass Spectrometry. The spots of individual digests, as well as chromatographic fractions, were analyzed both by single mass spectrometry (MS) and by tandem mass spectrometry (MS/MS) in the Manitoba/Sciex prototype quadrupole/TOF (QqTOF) mass spectrometer (commercial model sold as QSTAR by Applied Biosystems/MDS Sciex, Foster City, CA) (*31*, *32*). In this instrument, ions are produced by irradiation of the sample with photon pulses from a 20 Hz nitrogen laser (VCL 337ND; Spectra-Physics, Mountain View, CA) with 300 mJ of energy per pulse. Orthogonal injection of ions from the quadrupole into the TOF section normally produces a mass resolving power of 10000 fwhm and accuracy within a few millidaltons in the TOF spectra in both MS and MS/MS modes. For MALDI analysis individual digests were mixed 1:1 with matrix solution, deposited on the target, and air-dried.

RESULTS

The identity of each preparation was confirmed by MS fingerprinting of tryptic fragments and by tandem MS of selected ions by MALDI QqTOF (see below). Integrin purity was assessed by SDS−PAGE and staining with Coomasie blue (Figure 1B). The functional activities of each of the integrins were determined in an ELISA-based assay by monitoring the binding of biotinylated fibronectin. All of the preparations displayed specific ligand binding that could be blocked by the presence of unlabeled ligand (Figure 1A).

Integrin Digestion and MS. Whole integrin preparations were digested in solution such that fragments from both the α and β chains would be expected in the digest. However, the unreduced β chains were relatively resistant to digestion (data not shown). Following reduction and alkylation fragments from both chains were readily detectable. Preliminary studies had determined that the amino acid sequence coverage of the integrins was incomplete unless the proteins were deglycosylated. As the integrins are predicted to contain only N-linked glycosylation, the proteins were treated with PGNase F to remove the glycans (*33*). This treatment resulted in the conversion of the asparagines that were the site of the carbohydrate linkage to an aspartic acid.

The mass spectrum of the digest of fully reduced, alkylated, and deglycosylated α5β1 results in a very complex pattern (Figure 2A). As indicated above, deglycosylation was required in order to acquire better coverage of the integrins. An example of effects of deglycosylation is given for the

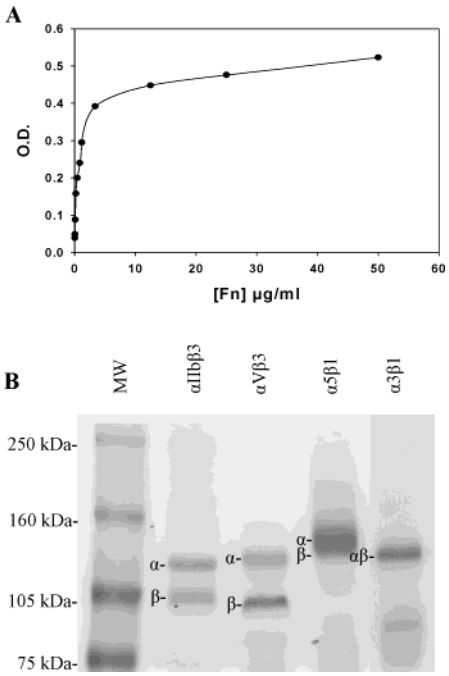

FIGURE 1: Characterization of integrin preparations. (A) Ligand binding by purified α5β1. Immobilized integrin (0.1 μg/well) was incubated with the indicated concentrations of biotinylated fibronectin, and the binding was quantitated following reaction with alkaline phosphatase conjugated streptavidin. The levels of nonspecific binding were assessed by determining the amount of ligand binding in the presence of a 100-fold excess of unlabeled fibronectin. Similar binding curves were generated for each of the purified integrins. (B) Coomasie blue staining of SDS−PAGE-separated reduced αIIbβ3, αVβ3, α5β1, and α3β1 and molecular mass markers (MW). The positions of the respective α and β chains are indicated for each integrin complex. In the case of α3 and β1 both chains comigrate as they have similar molecular masses.

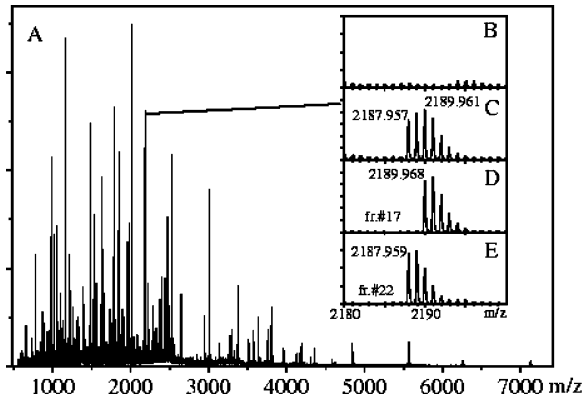

FIGURE 2: MALDI QqTOF MS spectra of the α5β1 integrin tryptic digest and μ-LC-MS analysis of the peptide mixture. (A) Mass spectrum of an unfractionated deglycosylated α5β1 integrin digest in the 500−8000 Da mass range. (B, C) Mass spectra of the (B) nondeglycosylated and (C) deglycosylated α5β1 integrin digest in the 2180−2210 Da range. The monoisotopic masses of fragments are shown above each peak. (D, E) Mass spectra of two HPLC fractions in the same *m*/*z* range as shown in (B) and (C). Note that the overlapping peptides in (C), *m*/*z* 2189.968 Da corresponding to deglycosylated β1(203−220) lrnpctseqDctspfsyk and *m*/*z* 2187.959 Da corresponding to deglycosylated α5(709−727) hpgDfsslscdyfavDqsr fragments, have been fully resolved into different fractions. D indicates Asn residues converted into Asp during deglycosylation with PNGase F.

region corresponding to the 2180−2210 Da *m*/*z* range before (Figure 2B) and after (Figure 2C) deglycosylation. The complexity of such samples as demonstrated in Figure 2C can be significantly reduced following off-line C18 μ-LC (Figure 2D,E). In this example the overlapping peaks in Figure 2C were resolved into two peaks that eluted in different fractions (i.e., fractions 17 and 22). The peak with *m*/*z* 2189.968 Da (Figure 2D) corresponds to a β1(203−220)-derived peptide, and the fragment with *m*/*z* 2187.959 Da (Figure 2E) corresponds to α5(709−727). The resulting digest gave almost complete coverage after HPLC fractionation with full accessibility to the cysteine-containing fragments of the integrin chains.

Disulfide Assignments. MS assignment of disulfide bonds is generally achieved by comparing masses of nonreduced and reduced digest (or aliquots of digest) of a protein that was digested with intact disulfide bonds (*25*). Peptides with a single intrachain disulfide bond exhibit a 2 Da increase in mass associated with reduction of their half-cysteines. During MALDI analysis in the linear mode, in-source fragmentation, or prompt fragmentation, can occur at the disulfide bonds in the disulfide-bridged peptide fragment (*34*, *35*). This leads to the appearance of reduced forms of peptides on mass spectra of the disulfide bond containing parent ion, facilitating its direct assignment. We did not observe these phenomena in our experimental conditions on QqTOF instrument. Although instrument settings can be optimized to facilitate prompt fragmentation by increasing laser fluence (*34*), we were able to assign 29 disulfide pairs by direct MS measurements of the nonreduced and reduced/alkylated integrin digest or mass spectra of their HPLC fractions.

The approach for assigning disulfide-linked fragments was based on measurements of the masses of the integrin-derived tryptic fragments before and after reduction and alkylation. The appearance of new fragments following reduction and the consequent disappearance of the fragments corresponding to the predicted disulfide-linked peptides provided the basis for assigning bonding patterns. As a confirmation of these assignments, the amino acid sequences of each of the alkylated peptides were confirmed by MS/MS. This approach, in conjunction with the homology-based assignments of disulfide bonds, allowed for the rapid selection of candidate peptides for analysis.

The spectra in Figure 3A,B demonstrate an example of fragments that contained a disulfide linking two peptides. In this case, a peptide with a mass of 3856.855 was observed in digests of nonreduced α5β1 (Figure 2A). In contrast, analysis of digests of reduced and alkylated α5β1 failed to display this fragment. However, two new species were detected with masses of 2307.127 (Figure 2B) and 1666.794 (data not shown). These correspond to the α5-derived tryptic fragments 864−878 and 921−939, respectively, in which the single cysteines in each fragment have been carboxamidomethylated, resulting in a mass increase of 57.021 per fragment. These results allowed for the unambiguous assignment of a disulfide bond between Cys 869 and Cys 921 present in these fragments.

In some cases, fragments contained an internal disulfide. A nonalkylated fragment of α5 with a mass of 952.365 was observed (Figure 3C). Following reduction and alkylation of the digested α5β1 integrin, this fragment disappeared, and a new species with a mass of 1068.438 was observed (Figure 3D). These results were consistent with the presence of an internally disulfide-bonded peptide in the native α5β1. This fragment corresponded to the predicted α5 peptide 911−918 (Table 1). Collectively these results indicated that the approach could be employed to examine integrin disulfide bonding patterns. On the basis of this information we performed a detailed analysis of the disulfide bonding patterns of the α chains of α3, α5, αV, and αIIb.

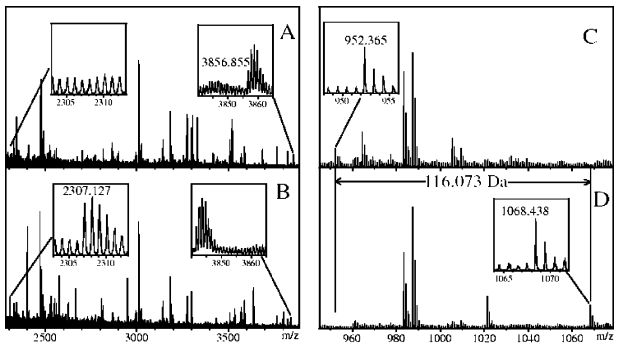

FIGURE 3: Mass spectra demonstrating disulfide assignment. (A, B) Example of mass shifts and disappearance of peak (3856.855) from spectra of (A) the unreduced α5β1 integrin digest and (B) the appearance of lower molecular mass fragments following reduction and alkylation (2307.127). Note that the other fragment (1666.794) was also observed, but it is below the *m*/*z* range of the spectrum presented in this figure. (C, D) Mass spectra of the α5β1 digest showing fragment 911−918 under (C) nonreduced and (D) reduced and alkylated conditions. Note the increase in mass due to the addition of two acetamides to the cysteines in this fragment.

A second strategy for disulfide bond assignment was based on the partial reduction of integrins followed by alkylation with iodoacetamide (*36*−*39*). The excess iodoacetamide was removed, and the integrins were fully reduced. The resultant free sulfydryl groups were alkylated with iodoacetic acid. Those fragments alkylated with iodoacetic acid displayed a mass shift 0.984 Da greater than those alkylated with iodoacetamide. The relative intensities of the peaks corresponding to iodoacetamide/iodoacetic acid alkylated peptides provided semiquantitative information about the degree of reduction under the mild reduction conditions. This approach based on MS measurements may be somewhat complicated for the fragments carrying more than one Cys. In the case of cysteines from the same peptide that display different sensitivities to reduction, additional MS/MS measurements were required to assign the actual position of the iodoacetamide-alkylated (e.g., reduced) Cys.

The spectra in Figure 4A,B illustrate this approach for an α5-derived peptide, 911−918. A peak of 1070.408 Da was observed in the fully reduced integrin sample following alkylation with iodoacetic acid (Figure 4A). However, under mild reduction conditions a peak with *m*/*z* 1068.441 appeared after alkylation with iodoacetamide (Figure 4B). These results indicate that a component of the integrins containing this disulfide pair was sensitive to mild reduction. This approach is particularly effective in combination with μ-HPLC fractionation prior to MALDI MS (MS/MS) analysis. μ-HPLC separation dramatically simplifies the MS spectra and provides at least a 10-fold increase in sensitivity (Figure 4C,D). In addition to this, peptides differentially alkylated with iodoacetamide/iodoacetic acid exhibit different chromatographic behavior: those alkylated with iodoacetamide always elute earlier from the RP C18 column (Figure 4D,

Table 1: Details of the MS-Based Assignments of Disulfide Bonding[a]

Cys residues	fragment(s)		calcd *m/z* alk pep	obsd *m/z* alk pep	calcd *m/z* unred. pep	obsd *m/z* unred. pep
		αIIb				
87−96	73−90	TLGPSQEETGGVFL***C***PWR	2033.975	2033.978	3479.672	3479.691
	91−104	AEGGQ***C***PSLLFDLR	1562.764	1562.762		
138−161	122−149	QGLGASVVSWSDVIVA***C***APWQHWNVLEK	3136.568	3136.589	5312.587	5316.7[A]
	150−170	TEEAEKTPVGS***C***FLAQPESGR	2293.077	2293.092		
177−198	172−178	AEYSP***C***R	882.378	882.384		
	197−307	Y***C***EAGFSSVVTQAGELVLGAPGGYYFLGLLAQAP VADIFSSYRPGILLWHVSSQSLSFDSSNPEYFDGYW GYSVAVGEFDGDLDTTEYVVGAPTWSWTLGAVEI LDSYYQR	12167.785			
504−(515, 521)−576	503−510	S***C***VLPQTK	932.448	932.459	5461.582	5465.0[A]
	511−532	TPVS***C***FNIQM***C***VGATGHNIPQK	2459.163	2459.175		
	572−590	HSPI***C***HTTMAFLRDEADFR	2304.065	2304.094		
633−639	629−692	IVLD***C***GEDDV***C***VPQLQLTASVTGSPLLVGADNVLE LQMDAANEGEGAYEAELAVHLPQGAHYMR	6849.280	2853.3 (av)	2733.221	6737.1[A]
705−718	703−708	LI***C***NQK	775.414	775.411	2046.091	2046.056
	715−726	VVL***C***ELGNPMKK	1387.744	1387.756		
857−(911, 916, 921)	811−876	VEHTYELHNDGPGTVDGLHLSIHLPGQSQPSDLLY ILDIQPQGGLQ***C***FPQPPVNPLK	6279.161	6281.9[A]	9037.405	9043.0[A]
	903−928	LQDPVLV***C***SDSAP***C***TVVQ***C***DLQEMAR	2991.368	2991.400		
		αV				
89−97	89−95	***C***DWSSTR	911.368	911.373	2201.934	2201.940
	97−108	***C***QPIEFDATGNR	1407.633	1407.639		
138−158	135−145	ILA***C***APLYHWR	1399.731	1399.726	2734.348	2734.352
	153−165	EPVGT***C***FLQDGTK	1451.684	1451.697		
172−185	166−173	TVEYAP***C***R	995.462	995.474	3271.431	3271.516
	174−195	SQDIDADGQGF***C***QGGFSIDFTK	2393.036	2393.038		
491−502	467−499	ARPVITVNAGLEVYPSILNQD***D***KT***C***SLPGTALK	3540.874	3540.880	4305.237	4305.198
	500−506	VS***C***FNVR	881.430	881.435		
508−565	507−510	F***C***LK	567.296		2866.357	2866.381
	560−579	GGLMQ***C***EELIAYLRDESEFR	2416.128	2416.127		
626−632	619−635	QAHILLD***C***GEDNV***C***KPK	1996.958	1996.951	1880.900	1880.918
698−711	696−701	LS***C***AFK	725.366	725.361	1868.907	1868.915
	708−718	VV***C***DLGNPMK	1260.608	1260.600		
852−914	833−862	YN***D***NTLLYILHYDIDGPM***DC***TSDMEINPLR	3601.63	3601.63	4316.014	4316.03
	912−918	IV***C***QVGR	831.451	831.460		
904−909	891−911	DLALSEGDIHTLG***C***GVAQ***C***LK	2257.096	2257.100	2141.037	2141.043
		α3				
94−103	88−105	TGAVYL***C***PLTAHKDD***C***ER	2105.975	2105.978	1989.916	1989.909
140−162	137−143	VLV***C***AHR	854.467	854.466	1334.682	1334.676
	162−165	***C***YVR	597.282	597.284		
185−197	166−221	DLELDSSDDWQTYHNEM***C***NSNTDYLETGM***C***QLG TSGGFTQNTVYFGAPGAYNWK	6359.655	6364.5[A]	6243.596	6248.5[A]
(485, 490, 496)−550	472−509	TLVPRPAVLDPAL***C***TATS***C***VQVEL***C***FAY***D***QSAGNP NYR	4254.042	4254.037	5666.795	5672.4[A]
	550−562	***C***QKLELLLMDNLR	1645.877	1645.851		
615−621	590−628	SLDAYPILNQAQALE***D***HTEVQFQKE***C***GPDNK***C***ES NLQMR	4577.114	4577.124	4461.055	4461.057
694−702	666−710	SGEDAHEALLTLVVPPALLLSSVRPPGA***C***QA***D***ETIF ***C***ELGNPFKR	4875.481	4875.483	4759.422	4759.348
846−904	829−872	WLLYPTEITVHGNGSWP***C***RPPGDLINPLNLTLSDP GDRPSSPQR				
	898−908	SETVLT***C***ATGR	1194.579	1194.580		
911−916	909−930	AH***C***VWLE***C***PIPDAPVVT***D***VTVK	2506.247	2506.245	2390.189	2390.183
		α5				
99−108	83−116	A***D***TSPGVLQGGAVYL***C***PWGASPTQ***C***T PIEFDSK	3637.694	3637.682	3521.635	3521.635
156−176	148−163	AHGSSILA***C***APLYSWR	1788.886	1788.874	4202.98	4203.013
	164−185	TEKEPLSDPVGT***C***YLSTD***D***FTR	2531.161	2531.173		
192−205	186−193	ILEYAP***C***R	1021.514	1021.519	3305.467	3305.495
	194−215	SDFSWAAGQGY***C***QGGFSAEFTK	2401.02	2401.019		
(513, 522, 528)−584	512−534	S***C***SLEGNPVA***C***I***D***LSF***C***L***D***ASGK	2500.116	2500.120	4844.266	4844.281
	567−588	QATLTQTLLIQNGARED***C***REMK	2576.293	2576.312		
645−651	639−694	AQILLD***C***GEDNI***C***VPDLQLEVFGEQNHVYLGDKN AL***D***LTFHAQNVGEGGAYEAELR	6257.982	6257.921	6141.924	6141.995
718−731	709−727	HPG***D***FSSLS***C***DYFAV***D***QSR	2187.941	2187.942	3330.523	3330.535
	728−738	LLV***C***DLGNPMK	1259.649	1259.649		
849−957	814−863	DQPQKEEDLGPAVHHVYELINQGPSSISQGVELS***C*** PQALEGQQLLYVTR	5570.787	5570.764	7189.531	7189.639
	949−962	EHQPFSLQ***C***EAVYK	1735.811	1735.808		

Table 1 (Continued)

Cys residues	fragment(s)		calcd *m/z* alk pep	obsd *m/z* alk pep	calcd *m/z* unred. pep	obsd *m/z* unred. pep
		α5				
869−921	864−878	VTGL***DC***TTNHPINPK	1666.822	1666.794	3856.886	3856.855
	921−939	***C***ELGPLHQQESQSLQLHFR	2307.13	2307.127		
911−916	911−918	***C***PEAE***C***FR	1068.424	1068.458	952.365	952.365

[a] The table lists the calculated and observed *m/z* of the tryptic peptides, with (alk red.) or without (unred.) reduction and alkylation, of the indicated α chains that contain Cys. The superscript A indicates the average *m/z* of the MH^+; all other masses correspond to monoisotopic *m/z* values. The numbers in the first column indicate the residue numbers of the disulfide-bonded Cys. Disulfide-linked peptides are indicated by a brace. ***D*** indicates asparagine residues that are converted to aspartic acid as a result of deglycosylation with PGNase F. ***D*** indicates glutamine residues that were deamidated during the processing.

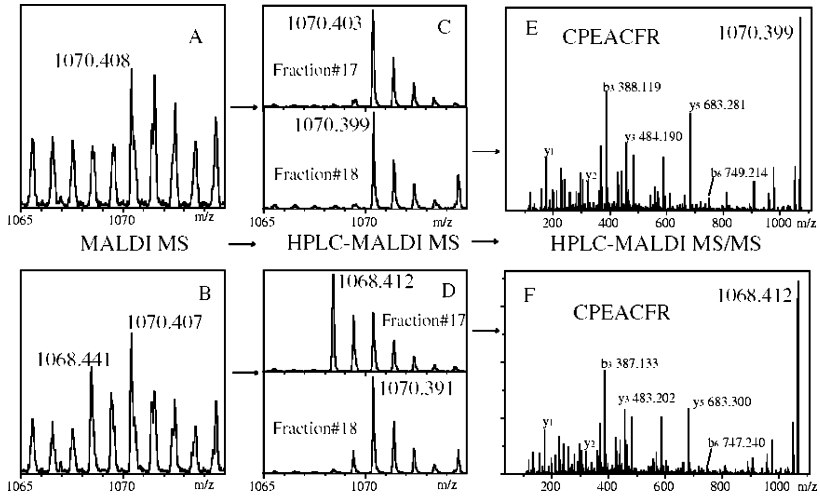

FIGURE 4: Example of MS (MS/MS) identification of disulfide bonds using differential iodoacetamide/iodoacetic acid alkylation. (A) MS spectra of the α5β1 integrin digest showing the 911−918 fragment completely alkylated with iodoacetic acid. (B) The same spectra of the α5β1 digest after reduction in mild conditions. The appearance of a new fragment with a mass shift of −1.966 Da relative to the 1070.407 Da peak indicates iodoacetamide alkylation (e.g., partial reduction) of two Cys residues. (C, D) Mass spectra of fractions 17 and 18 of the same digests shown in (A) and (B), respectively, collected after μ-HPLC fractionation. MS/MS spectra of the 1070.399 (E) and 1068.412 (F) Da peaks, confirming their respective alkylation with iodoacetic acid and iodoacetamide.

fractions 17 and 18). Subsequent MS/MS analysis (Figure 4E,F) confirmed complete alkylation of the 1070.399 Da fragment with iodoacetic acid or of the 1068.412 Da fragment with iodoacetamide. The simultaneous reduction of both cysteines in this fragment confirms our previous assignment of an internal disulfide bond on the α5 911−918 tryptic fragment. This approach was particularly useful in assigning possible disulfide pairs in fragments that contained multiple cysteines.

Tandem mass spectrometry provided a useful adjunct for the assignment of disulfide bonds. Depending on the peptide composition, fragments corresponding to cleavage of either the disulfide bridge or the peptide chain of the parent ion can be observed in the MS/MS spectra (*40*). We used MALDI MS/MS with low-energy collisionally induced dissociation to confirm our assignment for those disulfide-containing peptides with masses less than 4300 Da. An example of an MS/MS spectrum of a peptide with an intrachain bond α5(911−916) CPEAECFR is shown in Figure 5A. Although peptide bonds within disulfide loops of peptides are resistant to gas-phase fragmentation (*25*, *40*), we did observe a few fragments corresponding to cleavage between two Cys in the reduced peptide (b2 and b3 shown). The daughter ions carrying the intact −S−S− bridge (b6) were also observed. These observations are consistent with possible in-source prompt fragmentation (*34*). However, this appears to only occur to a very small extent as the b3 fragment is the dominant species in the MS/MS spectra of the fully reduced and alkylated α5(911−916) fragment (Figure 4E,F).

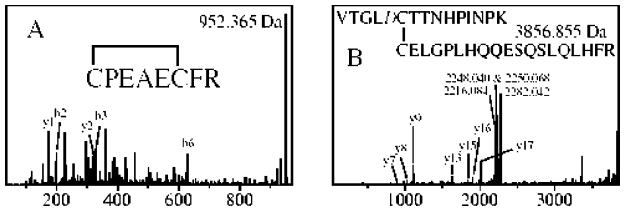

FIGURE 5: Direct MS/MS detection of the α5 integrin fragments containing disulfide bonds. (A) MS/MS spectra of the α5(911−916) CPEAECFR tryptic peptide, carrying an internal disulfide bond. Several daughter ions are labeled, including the b2 and b3 fragments formed due to S−S bond in-source cleavage. (B) MS/MS spectra of the 3856.855 Da peptide, carrying an interchain disulfide bond, which was not assigned previously on the basis of homology. The most intensive daughter ions correspond to the −S−S− bridge cleavage (2216.084−2248.040 and 2250.068−2282.042 Da). Several prominent y fragments from the α5(921−939) peptide are labeled.

A characteristic triplet of intense fragment ions dominates the MS/MS spectra of interchain disulfide-linked peptides in both the collisionally induced dissociation (*40*) and post source decay (*35*) modes. These arise as a result of fragments with a mass separation of 32−34 Da generated by −S−S− bond cleavage, corresponding to the retention of zero, one, or two sulfurs on the charged fragments. The MS/MS

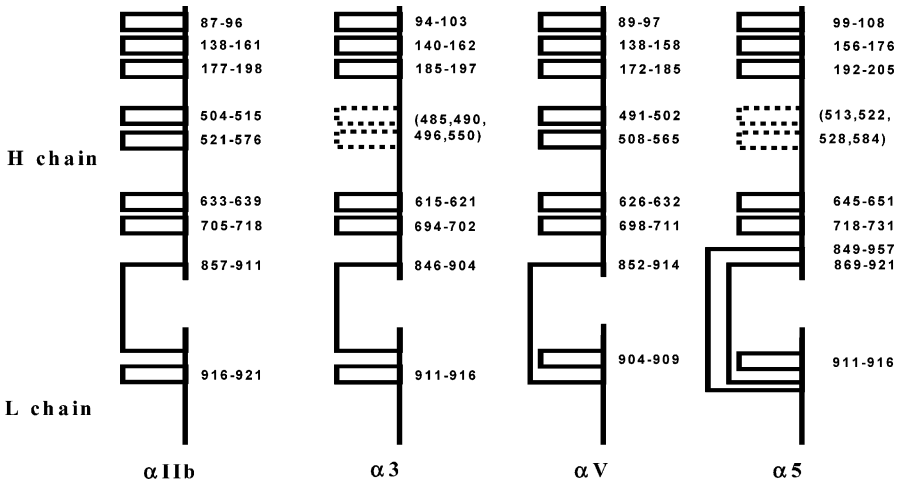

FIGURE 6: Schematic representation of the disulfide bonding pairings proposed for αIIb, α3, αV, and α5. The leftmost schematic outlines the predicted disulfide bonding patterns described by Calvette et al. for αIIb. The remaining schematics indicate the disulfide bonding patterns determined in the present study. Dashed bonds indicate patterns which were not assignable in this study. H and L indicate integrin α heavy and light chains, respectively. The α5 Cys849−Cys957 pair represents a previously unassigned set of bonds.

spectrum of a 3856.855 Da fragment carrying an interchain disulfide 869−921 bond (Figure 5B) displays such a pattern. In addition to the characteristic triplet 2216.084−2248.040 and 2250.068−2282.042 Da, a series of y fragments from α5(921−939) were also identified (Figure 5B). A triplet, corresponding to the other chain of the disulfide-linked partner, α5(864−878), was not found due to low abundance.

α*IIβ*. This integrin represents the prototypic structure upon which the disulfide patterns of all integrin α chains are assigned (19). As a test of the approach, the disulfide bonding patterns of αIIbβ3 were examined by mass spectrometry.

For five cysteine pairs it was possible to make clear assignments (cysteines 87−96, 138−161, 177−198, 633−639, and 705−718). These results were in agreement with the previous assignments in αIIb (*19*). The remaining cysteines were not assignable to specific bonding partners because the tryptic fragments contained multiple cysteines (Table 1). For example, in peptides from native integrin, a fragment with an average mass of 5465.0 was observed. However, this peak was absent in the reduced and alkylated digests of integrins, and three new fragments were detected. These corresponded to peptides 503−510, 511−532, and 572−590. The 511−532 peptide contains two cysteines. Similarly, peptide 903−928 contains three cysteines, one of which is bonded to the cysteine in peptide 811−867. Under these conditions, an unequivocal assignment could not be made for the bond pairs.

Preliminary studies demonstrated that reduction of αIIbβ3 under mild conditions resulted in the exposure of a limited number of cysteines in the α chain. We therefore used the strategy of differential alkylation described in the previous section. Those fragments alkylated with iodoacetic acid displayed a mass shift 0.984 Da greater than those alkylated with iodoacetamide. Thus, the fragments that contained cysteines reduced under the mild conditions were mass shifted differently from the remaining cysteine-containing fragments. Using this approach only Cys 857 and Cys 911 were alkylated with iodoacetamide, indicating that these two residues formed a bond pair. The Cys 916−Cys 921 formed an internal disulfide bond in the 903−928 fragment. Collectively, these results are in complete agreement with the previous assignments provided for this integrin (*19*) (Table 1, Figure 6).

α*V*. The αV chain has the same number of cysteines as αIIb, and both of these chains can pair with β3 to bind an overlapping set of ligands (e.g., fibronectin), suggesting a very high degree of structural and functional homology (*41*). All of the disulfide bonds could be assigned for αV (Table 1). The first seven pairs were homologous to those reported for αIB. However, the pairing for the remaining cysteines differed from those suggested for αIIb.

The αV fragment, 891−911, contains two cysteines, 904 and 909, which based on homology with αIIb are predicted to be involved with disulfide bonds with cysteines 852 and 914, respectively. No evidence was found for such an association. In fact, the results indicated the presence of an internal disulfide bond in this peptide (Table 1). Furthermore, fragments consistent with a Cys 852 −Cys 914 pairing were observed. These results suggested that the αV bonding pattern was not fully homologous with those reported for αIIb (Table 1, Figure 6).

α*3*. The α3 chain pairs with the β1 integrin chain to generate a receptor for collagen and fibronectin, but it displays structural and posttranslational modification properties similar to those of αIIb and αV (*42*). It was therefore questioned what the disulfide patterns of this integrin would be. It was possible to fully assign seven of the nine disulfide bonds. The remaining two bonds involved peptides 472−509 and 550−562. The former peptide contains three cysteines, which precluded specific assignment of the residues involved in bonding to the cysteine in the 550−562 peptide.

The C-terminal region of the α3 corresponding to the area where αV and αIIb bonding patterns differed was readily resolvable. The α3 chain displayed disulfide patterns (i.e., Cys 846−Cys 904 and Cys 911−Cys 916) that were homologous with αIIb (Table 1, Figure 6).

α*5*. This chain pairs with the β1 integrin chain to generate the classical fibronectin receptor (*43*). The α5 chain contains two additional cysteines (i.e., a total of 20) that are not present in the other α chains reported above. The bonding patterns of these cysteines have not been determined, and

they could not be assigned on the basis of homology with αIIb.

Cysteines 849 and 957 are nonhomologous. These were paired with one another to generate a bond between sequentially distant regions of the integrin molecule. The pairing patterns of the remaining cysteines were all assignable except for four that were present in two fragments corresponding to residues 512−534 and 567−584. The former fragment contained three cysteines, which prevented the assignment of the residues involved in the interfragment bonding pair.

The pairing of Cys 869−Cys 921 and Cys 911−Cys916 was observed in the carboxyl-terminal region of this chain. Although these are the homologues of the four C-terminal cysteines in αIIb, these residues displayed a pattern that was similar to that observed for αV (Table 1, Figure 6).

DISCUSSION

Our results provide several new insights into integrin disulfide bonding in particular and in bonding assignments in general. The patterns of four integrin α chains (αIIb, αV, α3, α5) are described. The α chains display differences in the disulfide patterns of those bonds near their C-terminal regions linking the heavy and light chains. Also, the location of a previously unassigned disulfide pair is provided for α5. The results point out the limitations of homology-based bonding assignment within a family of molecules.

All of the α chains examined in this study undergo posttranslational cleavages near the C-terminus to generate disulfide-linked heavy (H) and light (L) chains (*2*). The L chains contain transmembrane and cytoplasmic sequences. These serve to anchor the integrins to the cell surface. The prototypic integrin has been αIIbβ3 as it was the first member of the family in which full assignment of disulfide bonds was made (*19*, *20*). The disulfide bonds of other integrin α chains are assigned by homology with the αIIb. In those cases where the chain has more Cys than αIIb, the bonds were left unassigned. However, recent structural analysis of a soluble αVβ3 construct has raised some concerns about the generality of the αIIb assignments because different patterns of disulfide bonding were observed in the carboxyl-terminal regions of these two α chains (*21*, *22*). We undertook use of mass spectrometric based approaches to examine integrin bonding patterns with particular emphasis on the bonds linking the H and L chains.

Mass spectrometry has been used extensively to characterize disulfide bond patterns in proteins (reviewed in ref *25*). The possibility of disulfide rearrangements is a concern in any study of their bonding patterns. The proteins were reduced and alkylated under neutral to slightly acidic conditions in an effort to minimize the possibility of disulfide exchange during the separation. Given that there was an absence of free disulfides detected in native α chains, the probability of such a process is markedly reduced, but it cannot be absolutely ruled out at this point (*25*). The inclusion of a chromatographic step markedly reduced the complexity of the spectra of the digests. It also resulted in a lowering of the background, providing a better signal to noise ratio. This permitted the identification of almost all of the peaks expected to derive from the α chains. The identities of disulfide-linked peptides were predicted on the basis of MS determined masses and subsequently confirmed by MS/MS, allowing for high confidence in assignments of the half-cysteinyl pairs. The regions of the α chains containing the fourth and fifth cysteines proved to be particularly problematic for disulfide assignments because these regions contained multiple peptides which lacked tryptic cleavage sites. While cleavage approaches using other enzymes or chemical methods are potentially available to analyze this, the complexity of the glycosylation patterns in this region would result in complex spectra with dissipation of the sample between multiple peaks (*25*). However, this did not interfere with our ability to characterize the majority of the disulfide bonds and to detail those cysteines involved in the region near the heavy and light chain interface.

The patterns of all of the assigned disulfide bonds in the N-terminal regions of the α chains were similar to those reported for αIIb (i.e., those involving the first 14 cysteines). Similarly, the remainder of the disulfide bonds in αIIb (857−911 and 919−921) were identical to those previously described (*19*). The disulfide pattern observed for αV was different from that reported for αIIb (Figure 6). However, these results are consistent with those obtained for αV by crystallography (*21*). These observations validated the current approach and suggested that disulfide rearrangement was not occurring during the processing. Extension of the analysis to the α3 and α5 chains demonstrated that these differences were observed in other species of α chains. The α3 chain was similar to αIIb in bonding patterns. In the case of the fibronectin receptor, α5, the overall organization was similar to that observed for αV (Figure 6). However, unlike the other integrins in this study this α chain has an additional pair of cysteines that had not been previously assigned. This pair was shown to link the H and L components of the α5 chain. These results indicate that not all integrin species display an identical bonding pattern of homologous cysteines.

The α5β1 complex binds to fibronectin, and it has been shown to have a primary role in fibronectin matrix assembly (*44*−*46*). Integrin binding of dimeric fibronectin is a primary event in the assembly of initially detergent-soluble fibrils into an insoluble matrix (*44*). It is unclear whether this process is mediated by disulfide exchange or protein−protein interactions involving newly exposed sites. Both fibronectin and integrins have been shown to express endogenous thiol isomerase activity that could facilitate the former process through disulfide exchange during fibronectin fibril generation (*16*, *47*). It is conceivable that the α5 chain may contribute to this process through the nonhomologous disulfide bond.

Recent evidence indicates a requirement for redox reactions in the control of αIIbβ3 integrin function (*18*, *48*). In these cases the β3 chain was found to exhibit an increase in the number of accessible free sulfydryl groups on activation of integrin function. The integrins examined in the present studies were functional, as demonstrated by their capacities to bind soluble ligand. Thus, it appears that the differences in disulfide bonding patterns of the α chains are not related to their ligand binding capacity. However, there have been several reports suggesting different affinity states for integrins, and it is possible that this may be the basis for the apparent heterogeneity in bonding patterns observed in the different integrin preparations. In the case of αIIbβ3 it is estimated that approximately 5% of the integrin isolated from

platelets is in a high-affinity state. Studies by Yan and Smith provided evidence for a correlation between integrin affinity state and disulfide rearrangement (*17*). Although the present studies were not specifically designed to determine the possible levels of microheterogeneity in the integrins, the results suggest that if there is microheterogeneity in the integrin preparations, the predominant species are those forms reported in the current study.

The results of this study also demonstrate the utility of mass spectrometry in the analysis of complex protein structures. While multiple proteases and protein separation may be required to obtain full coverage of the molecules, this is compensated for by the small amounts of protein needed and the generality of the approach.

ACKNOWLEDGMENT

We thank Sheryl Hagenstein for assistance in the preparation of the manuscript.

REFERENCES

1. Hynes, R. O. (2002) Integrins: bidirectional, allosteric signaling machines, *Cell 110*, 673−687.
2. Hemler, M. E. (1990) VLA proteins in the integrin family: structures, functions, and their role on leukocytes, *Annu. Rev. Immunol. 8*, 365−400.
3. Stupack, D. G., and Cheresh, D. A. (2002) Get a ligand, get a life: integrins, signaling and cell survival, *J. Cell Sci. 115*, 3729−3738.
4. McEver, R. P. (2001) Adhesive interactions of leukocytes, platelets, and the vessel wall during hemostasis and inflammation, *Thromb. Haemostasis 86*, 746−756.
5. Johnston, B., and Butcher, E. C. (2002) Chemokines in rapid leukocyte adhesion triggering and migration, *Semin. Immunol. 14*, 83−92.
6. Dustin, M. L., and Colman, D. R. (2002) Neural and immunological synaptic relations, *Science 298*, 785−789.
7. van Kooyk, Y., and Figdor, C. G. (2000) Avidity regulation of integrins: the driving force in leukocyte adhesion, *Curr. Opin. Cell Biol. 12*, 542−547.
8. Kucik, D. F., Dustin, M. L., Miller, J. M., and Brown, E. J. (1996) Adhesion-activating phorbol ester increases the mobility of leukocyte integrin LFA-1 in cultured lymphocytes, *J. Clin. Invest. 97*, 2139−2144.
9. Hogg, N., and Leitinger, B. (2001) Shape and shift changes related to the function of leukocyte integrins LFA-1 and Mac-1, *J. Leukocyte Biol. 69*, 893−898.
10. Liddington, R. C., and Ginsberg, M. H. (2002) Integrin activation takes shape, *J. Cell Biol. 158*, 833−839.
11. Davis, G. E., and Camarillo, C. W. (1993) Regulation of integrin-mediated myeloid cell adhesion to fibronectin: influence of disulfide reducing agents, divalent cations and phorbol ester, *J. Immunol. 151*, 7138−7150.
12. Edwards, B. S., Curry, M. S., Southon, E. A., Chong, A. S., and Graf, L. H., Jr. (1995) Evidence for a dithiol-activated signaling pathway in natural killer cell avidity regulation of leukocyte function antigen-1: structural requirements and relationship to phorbol ester- and CD16-triggered pathways, *Blood 86*, 2288−2301.
13. Peerschke, E. I. (1995) Regulation of platelet aggregation by post-fibrinogen binding events. Insights provided by dithiothreitol-treated platelets, *Thromb. Haemostasis 73*, 862−867.
14. Ni, H., Li, A., Simonsen, N., and Wilkins, J. A. (1998) Integrin activation by dithiothreitol or Mn2+ induces a ligand-occupied conformation and exposure of a novel NH2-terminal regulatory site on the beta1 integrin chain, *J. Biol. Chem. 273*, 7981−7987.
15. Lahav, J., Gofer-Dadosh, N., Luboshitz, J., Hess, O., and Shaklai, M. (2000) Protein disulfide isomerase mediates integrin-dependent adhesion, *FEBS Lett. 475*, 89−92.
16. O'Neill, S., Robinson, A., Deering, A., Ryan, M., Fitzgerald, D. J., and Moran, N. (2000) The platelet integrin alpha IIb beta 3 has an endogenous thiol isomerase activity, *J. Biol. Chem. 275*, 36984−36990.
17. Yan, B., and Smith, J. W. (2001) Mechanism of integrin activation by disulfide bond reduction, *Biochemistry 40*, 8861−8867.
18. Yan, B., and Smith, J. W. (2000) A redox site involved in integrin activation, *J. Biol. Chem. 275*, 39964−39972.
19. Calvette, J. J., Henschen, A., and Gonzalez-Rodriguez, J. (1989) Complete localization of the intrachain disulfide bonds and the N-glycosylation points in the alpha-subunit of human platelet glycoprotein IIb, *Biochem. J. 261*, 561−568.
20. Calvette, J. J., Henschen, A., and Gonzalez-Rodriguez, J. (1991) Assignment of disulfide bonds in human platelet GPIIIa. A disulfide pattern for the beta-subunits of the integrin family, *Biochem. J. 274*, 63−71.
21. Xiong, J. P., Stehle, T., Diefenbach, B., Zhang, R., Dunker, R., Scott, D. L., Joachimiak, A., Goodman, S. L., and Arnaout, M. A. (2001) Crystal structure of the extracellular segment of integrin $\alpha V\beta 3$, *Science 294*, 339−345.
22. Xiong, J. P., Stehle, T., Zhang, R., Joachimiak, A., Frech, M., Goodman, S. L., and Arnaout, M. A. (2002) Crystal structure of the extracellular segment of integrin $\alpha 4V\beta 3$ in complex with an Arg-Gly-Asp ligand, *Science 296*, 151−155.
23. Glocker, M. O., Arbogast, B., and Deinzer, M. L. (1995) Characterization of Disulfide Linkages and Disulfide Bond Scrambling in Recombinant Human Macrophage Colony Stimulating Factor by Fast-Atom Bombardment Mass Spectrometry of Enzymatic Digests, *J. Am. Soc. Mass Spectrom. 6*, 638−643.
24. Yen, T. Y., Yan, H., and Macher, B. A. (2002) Characterizing closely spaced, complex disulfide bond patterns in peptides and proteins by liquid chromatography/electrospray ionization tandem mass spectrometry, *J. Mass Spectrom. 37*, 15−30.
25. Gorman, J. J., Wallis, T. P., and Pitt, J. J. (2002) Protein disulfide bond determination by mass spectrometry, *Mass Spectrom. Rev. 21*, 183−216.
26. Pitt, J. J., Da Silva, E., and Gorman, J. J. (2000) Determination of the disulfide bond arrangement of Newcastle disease virus hemagglutinin neuraminidase. Correlation with a beta-sheet propeller structural fold predicted for paramyxoviridae attachment proteins, *J. Biol. Chem. 275*, 6469−6478.
27. Gorman, J. J., Ferguson, B. L., Speelman, D., and Mills, J. (1997) Determination of disulfide bond arrangement of human respiratory syncytial virus attachment (G) protein by matrix-assisted laser desorption/ionization time of flight mass spectrometry, *Protein Sci. 6*, 1308−1315.
28. Wu, J., and Watson, J. T. (1997) A novel methodology for assignment of disulfide bond pairing in proteins, *Protein Sci. 6*, 391−398.
29. Wilkins, J. A., Li, A., Ni, H., Stupack, D. G., and Shen, C. (1996) Control of $\beta 1$ Integrin Function, *J. Biol. Chem. 271*, 3046−3051.
30. Ni, H., and Wilkins, J. A. (1998) Localisation of a novel adhesion blocking epitope on the human beta 1 integrin chain, *Cell Adhes. Commun. 5*, 257−271.
31. Loboda, A. V., Krutchinsky, A. N., Bromirski, M., Ens, W., and Standing, K. G. (2000) *Rapid Commun. Mass Spectrom. 14*, 1047.
32. Shevchenko, A., Loboda, A., Shevchenko, A., Ens, W., and Standing, K. G. (2000) MALDI quadrupole time-of-flight mass spectrometry: a powerful tool for proteomic research, *Anal. Chem. 72*, 2132−2141.
33. Maley, F., Trimble, R. B., Tarentino, A. L., and Plummer, T. H., Jr. (1989) Characterization of glycoproteins and their associated oligosaccharides through the use of endoglycosidases, *Anal. Biochem. 180*, 195−204.
34. Patterson, S. D., and Katta, W. (1994) Prompt fragmentation of disulfide-linked peptides during matrix-assisted laser desorption ionization mass spectrometry, *Anal. Chem. 66*, 3727−3732.
35. Jones, M. D., Patterson, S. D., and Lu, H. S. (1998) Determination of disulfide bonds in highly bridged disulfide-linked peptides by matrix-assisted laser desorption/ionization mass spectrometry with postsource decay, *Anal. Chem. 70*, 136−143.
36. Gray, W. R. (1993) Disulfide structures of highly bridged peptides: A new strategy for analysis, *Protein Sci. 2*, 1732−1748.
37. Fischer, W. H., Rivier, J. E., and Craig, A. G. (1993) In situ reduction suitable for matrix-assisted laser desorption/ionization and liquid secondary ionization using tris(2-carboxyethyl)phosphine, *Rapid Commun. Mass Spectrom. 7*, 225−228.
38. Bures, E. J., Hui, J. O., Young, Y., Chow, D. T., Katta, V., Rohde, M. F., Zeni, L., Rosenfeld, R. D., Stark, K. L., and Haniu, M. (1998) Determination of disulfide structure in agouti-related

protein (AGRP) by stepwise reduction and alkylation, *Biochemistry 37*, 12172−12177.
39. Qi, J., Wu, J., Somkuti, G. A., and Watson, J. T. (2001) Determination of the disulfide structure of sillucin, a highly knotted, cysteine-rich peptide, by cyanylation/cleavage mass mapping, *Biochemistry 40*, 4531−4538.
40. Bean, M. F., and Carr, S. A. (1992) Characterization of disulfide bond position in proteins and sequence analysis of cysteine-bridged peptides by tandem mass spectrometry, *Anal. Biochem. 201*, 216−226.
41. Suzuki, S., Argraves, W. S., Arai, H., Languino, L. R., Pierschbacher, M. D., and Ruoslahti, E. (1987) Amino acid sequence of the vitronectin receptor alpha subunit and comparative expression of adhesion receptor mRNAs, *J. Biol. Chem 262*, 14080−14085.
42. Takada, Y., Murphy, E., Pil, P., Chen, C., Ginsberg, M. H., and Hemler, M. E. (1991) Molecular cloning and expression of the cDNA for alpha 3 subunit of human alpha 3 beta 1 (VLA-3), an integrin receptor for fibronectin, laminin, and collagen, *J. Cell Biol. 115*, 257−266.
43. Argraves, W. S., Suzuki, S., Arai, H., Thompson, K., Pierschbacher, M. D., and Ruoslahti, E. (1987) Amino acid sequence of the human fibronectin receptor, *J. Cell Biol. 105*, 1183−1190.
44. Schwarzbauer, J. E., and Sechler, J. L. (1999) Fibronectin fibrillogenesis: a paradigm for extracellular matrix assembly, *Curr. Opin. Cell Biol. 11*, 622−627.
45. Wu, C. (1997) Roles of integrins in fibronectin matrix assembly, *Histol. Histopathol. 12*, 233−240.
46. Wennerberg, K., Lohikangas, L., Gullberg, D., Pfaff, M., Johansson, S., and Fassler, R. (1996) Beta 1 integrin-dependent and -independent polymerization of fibronectin, *J. Cell Biol. 132*, 227−238.
47. Langenbach, K. J., and Sottile, J. (1999) Identification of protein-disulfide isomerase activity in fibronectin, *J. Biol. Chem. 274*, 7032−7038.
48. Essex, D. W., and Li, M. (2003) Redox control of platelet aggregation, *Biochemistry 42*, 129−136.

BI034726U